Supporting Information for

Ce(III) Yldiide Complexes with Divergent CO Reactivity

Alexander J. Gremillion,[a] Hemant Kumar,[a] Iker Del Rosal,[b] Steven P. Kelley,[a] Laurent Maron,[b] Viktoria H. Gessner,*[c] and Justin R. Walensky*[a]

[a] Department of Chemistry, University of Missouri, Columbia, MO 65211 USA, Email: walenskyj@missouri.edu

[b] Universite de Toulouse and CNRS, INSA, UPS, CNRS, UMR, UMR 5215, LPCNO 135 Avenue de Ranguiel, 31077 Toulouse (France), Email: laurent.maron@irsamc.ups-tlse.fr

[c] Faculty of Chemistry and Biochemistry, Ruhr-University Bochum, 44801 Bochum, Germany, Email: viktoria.gessner@rub.de

Table of Contents

General Considerations: All syntheses were carried out under an N_2 atmosphere using glovebox and Schlenk techniques unless otherwise stated. All solvents used were dried by passing through a solvent purification system (MBraun, USA). Benzene-d_6 (Cambridge Isotope Laboratories) was degassed by three freeze−pump−thaw cycles and stored over a potassium mirror. $[(C_5Me_5)_2CeCl_2K(THF)]$[1], $PhCH_2K$[2], $Ph_3PC(H)P(=S)Ph_2$[3], and $Ph_3PC(H)SO_2Tol$[4] were synthesized as reported. All ^1H and $^{13}C\{^1H\}$ spectra were taken on 600 or 300 MHz Bruker spectrometers. All NMR chemical shifts are reported in ppm. ^1H NMR chemical shifts were referenced internally to the residual solvent peak of C_6D_6 at 7.16 ppm. ^{13}C NMR chemical shifts were referenced internally to C_6D_6 at 128.06 ppm. IR was taken on a Nicolet Summit Pro FTIR spectrometer in transmission mode with a KBr pellet. Elemental analysis was performed at the University of Missouri, Columbia on a Carlo Erba 1108 elemental analyzer, outfitted with an A/D converter for analysis using Eager Xperience software.

Caution! Strong bases such as organolithium or potassium bases, especially as neat compounds, are severely air-/moisture-sensitive and pyrophoric organometallic compounds. These compounds need to be handled under an inert gas atmosphere to exclude reactions with oxygen and water. Guidelines for their handling can be found in literature: T. L. Rathman, J. A. Schwindeman, *Org. Process Res. Dev.* **2014**, *18*, 1192.

Caution! Carbon monoxide (CO) is a highly toxic gas. Reactions should be performed in well-ventilated fume hoods, ideally with a CO sensor.

Synthesis of [(C_5Me_5)$_2$Ce(κ^2-(C,S)-C(PPh_3){P(S)Ph_2})], 1. [(C_5Me_5)$_2$CeCl_2K(THF)] (100 mg, 0.169 mmol) was dissolved in toluene (10 mL) and added to a 20 mL scintillation vial. Separately, **1-H** (83 mg, 0.169 mmol) was dissolved in toluene (2 mL), yielding a light-yellow solution. To this was added a suspension of benzyl potassium in 2 mL of toluene (23 mg, 0.175 mmol). After 20 minutes of stirring, a color change from light-yellow to red was observed along with a clear appearance, with minimal undissolved benzyl potassium still visible. This solution was filtered through Celite to yield a clear red solution and was added slowly to the stirring vial of [(C_5Me_5)$_2$CeCl_2K(THF)]. After stirring at room temperature for 6 h, the reaction mixture was filtered through a fine porosity frit. The solvent was removed under reduced pressure, and the remaining red solid was extracted in toluene and filtered again through a Celite-containing pipet. Toluene was evaporated under a vacuum to obtain a pinkish-red-coloured solid compound **1**. If remaining ylide **1-H** is observed, then an equivalent amount (with respect to the remaining ylide) of benzyl potassium followed by the addition of an equivalent amount of [(C_5Me_5)$_2$CeCl_2K(THF)] can be added to the impure reaction mixture followed by filtration to get the analytically pure compound **1**. Single crystals of compound **1** (0.111 mg, 73%), suitable for the X-ray diffraction studies, were grown from its concentrated solution in toluene or THF with a few drops of diethyl ether after cooling at −20 °C for 16 hours. ^{1}H NMR (C_6D_6, 600 MHz, 298 K): 4.27 (s, 30H, C_5Me_5), 8.05 (t, 2H, [P(S)Ph_2]), 8.19 (bs, 4H, [P(S)Ph_2]), 9.64 (bs, 4H, [P(S)Ph_2)]. ^{13}C{^{1}H } NMR (C_6D_6, 150 MHz, 298K): 128.34 (s, C_5Me_5), 128.57 (s, Ph_3P), 128.6 (s, Ph_2P), 131.06 (s, Ph_2P), 131.37 (s, Ph_3P), 133.60 (bs, PPh_3), 136.48 (s, Ph_2P), 191.60 (bs, *ipso*-Ph_2P(S)P). Elemental analysis calculated for $C_{51}H_{55}CeP_2S$: (902.11 g/mol): C, 67.90%; H 6.15%; S, 3.55%. Found: C, 67.72%; H, 6.45%; S, 3.66%.

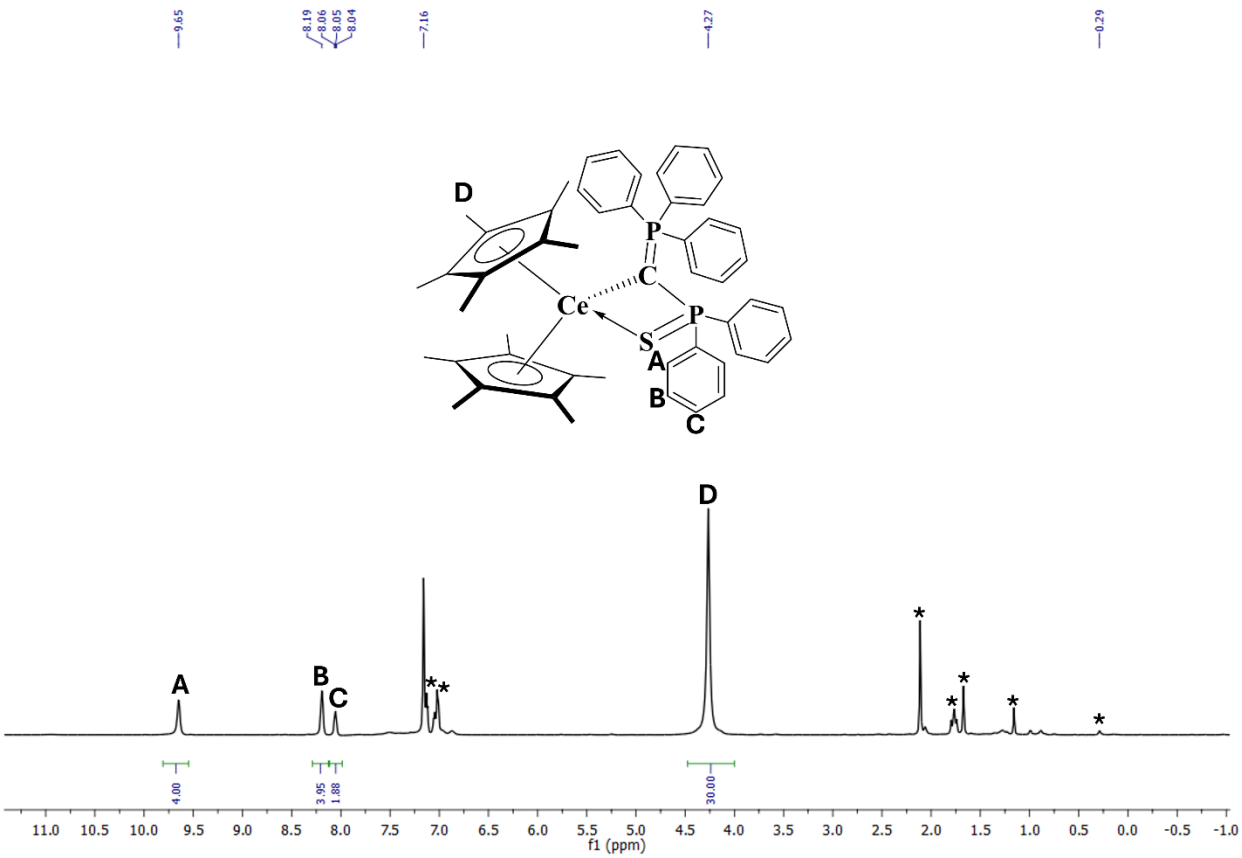

Figure S2: ^{1}H NMR (600 MHz, C_6D_6 298 K) of **1**, solvent impurities are present (toluene, *n*-pentane, silicon grease).

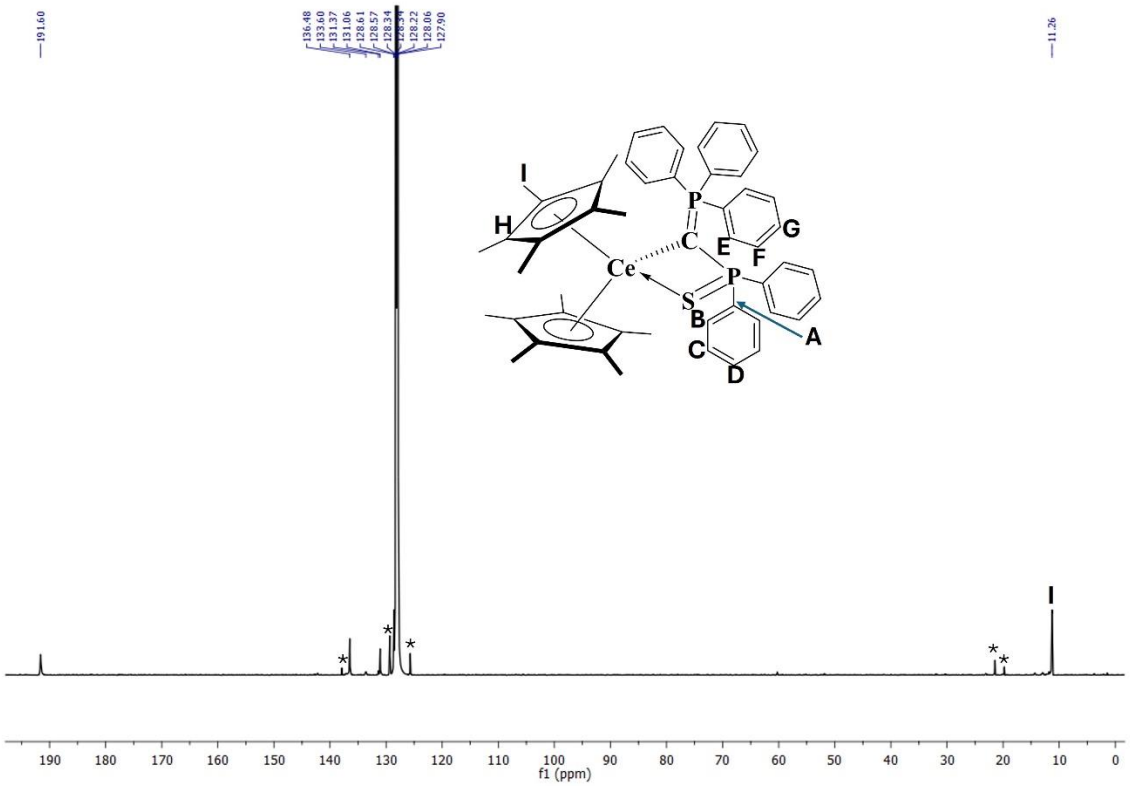

Figure S2: $^{13}C\{^{1}H\}$ NMR (150 MHz, C_6D_6 298 K) of **1**, solvent impurities are present (toluene, n-pentane).

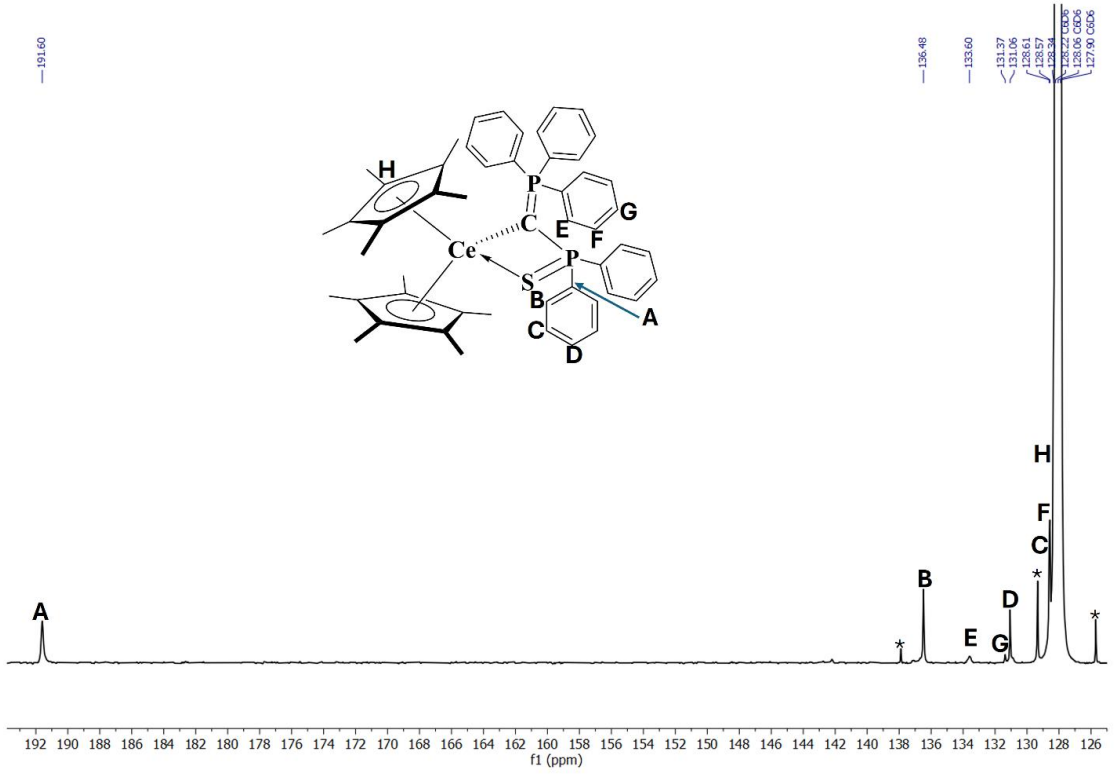

Figure S3: $^{13}C\{^{1}H\}$ NMR (150 MHz, C_6D_6 298 K) of **1**, aromatic region magnification, solvent impurities are present (toluene).

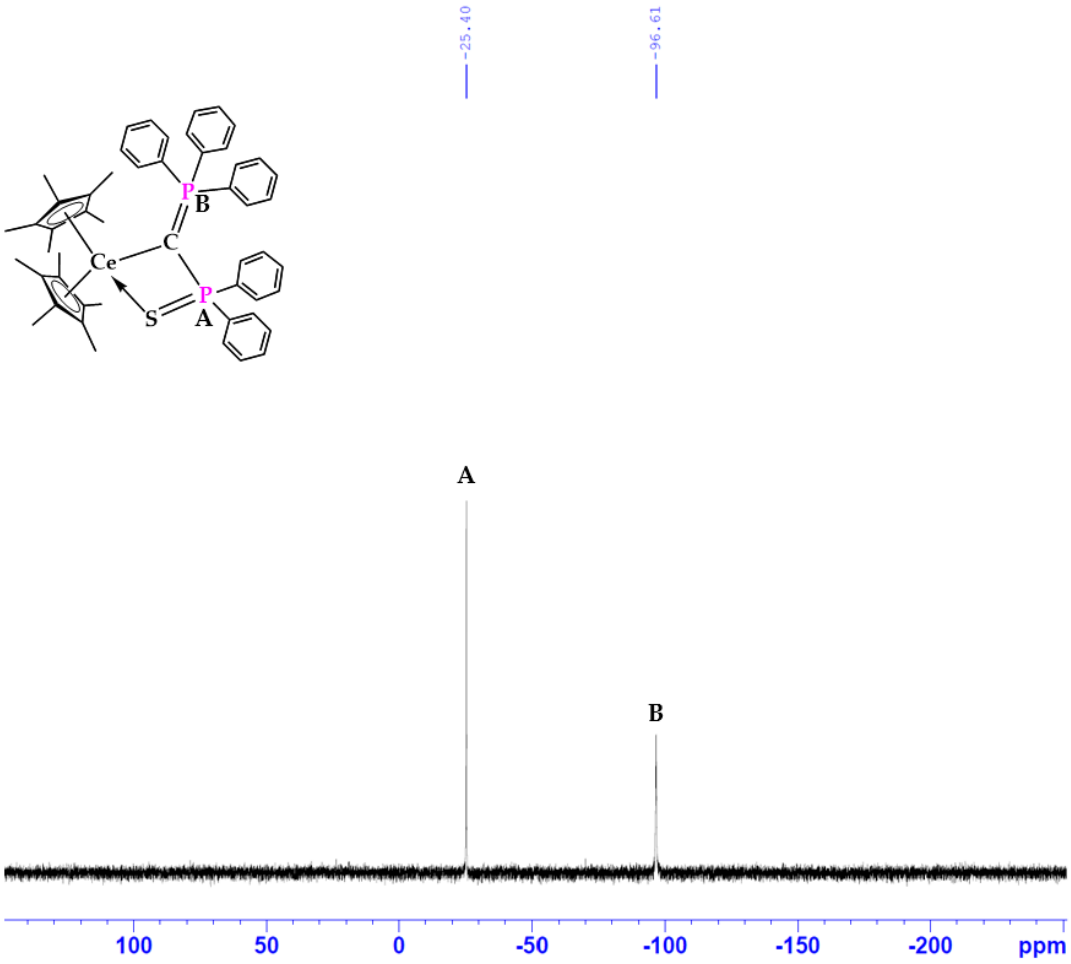

Figure S4: $^{31}P\{^{1}H\}$ NMR (250 MHz, C_6D_6 298 K) of **1**.

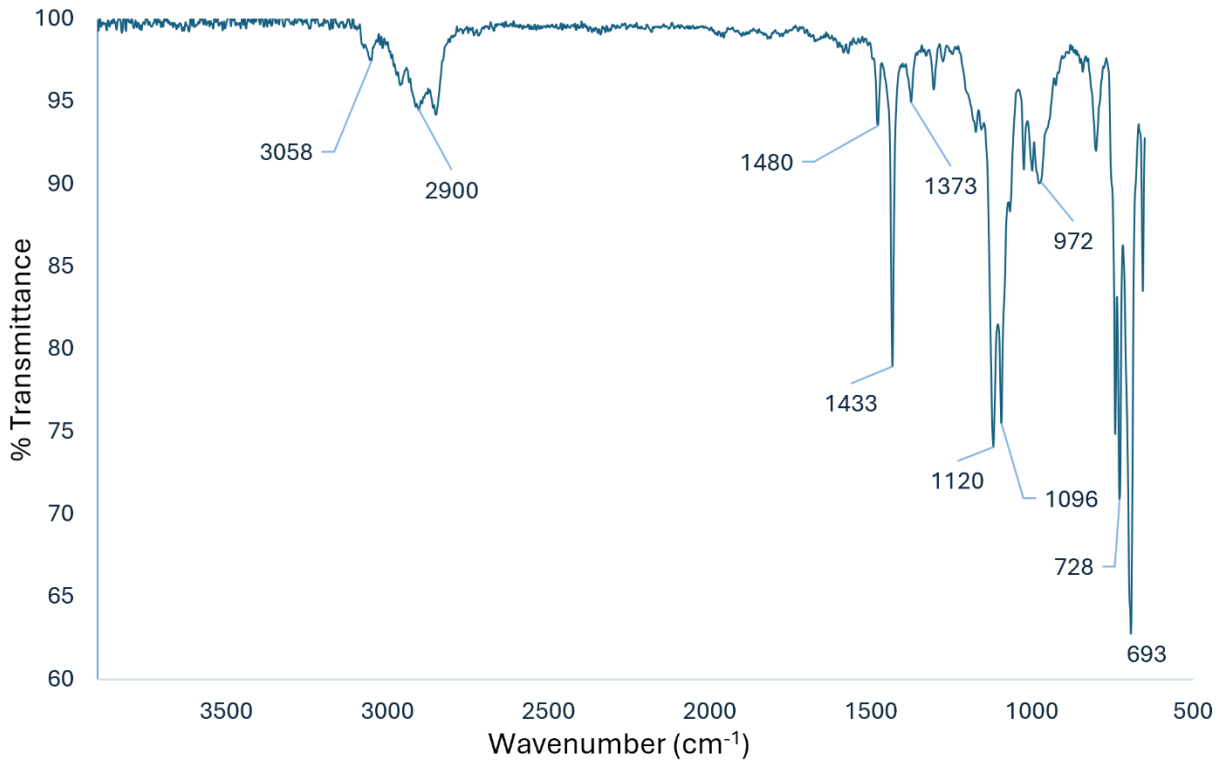

Figure S5: FT-IR vibrational spectrum of **1**, obtained using ATR.

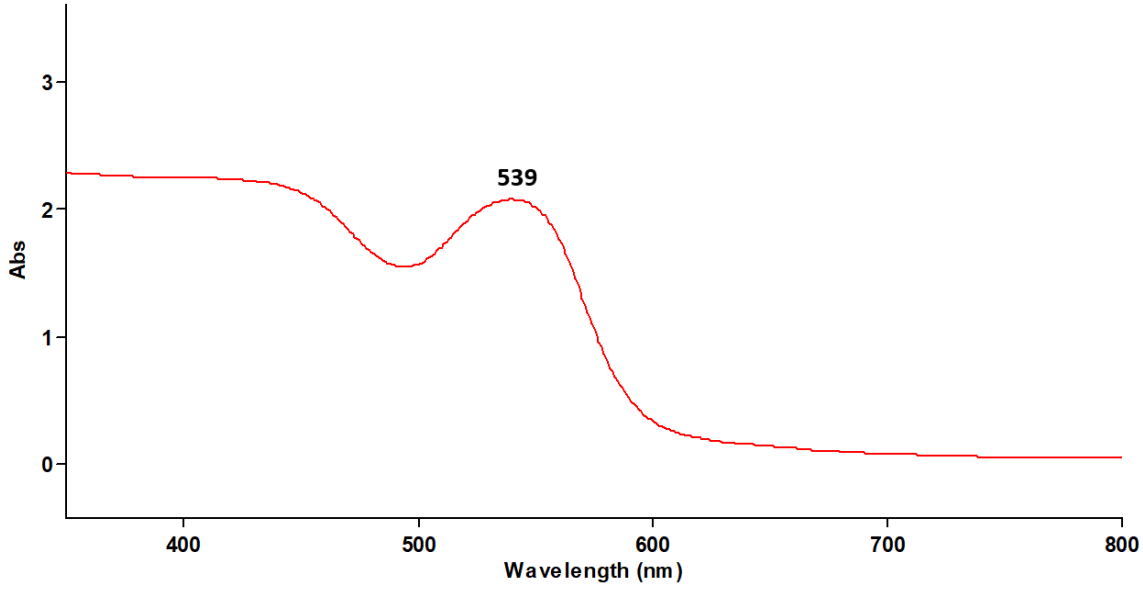

Figure S6: UV-vis spectrum of **1** (10 mM) collected in *n*-pentane with background subtraction.

Synthesis of [(C_5Me_5)$_2$Ce(κ^2-(C,O)-C(PPh_3){(SO_2PhMe})], (2). [(C_5Me_5)$_2$$CeCl_2$K(THF)] (120 mg, 0.202 mmol) was dissolved in toluene (10 mL) and added to a 20 mL scintillation vial. Separately, C(H)(PPh_3)(SO_2PhMe) (95 mg, 0.202 mmol) was dissolved in toluene (2 mL), yielding a light-yellow solution. To this was added a suspension of benzyl potassium in 2 mL of toluene (28 mg, 0.208 mmol). After 20 minutes of stirring, a color change from light-yellow to red was observed along with a clear appearance, with minimal undissolved benzyl potassium still visible. This solution was filtered through celite to yield a clear red solution and was added slowly to the stirring vial of [(C_5Me_5)$_2$$CeCl_2$K(THF)]. After stirring at room temperature for 6 h, the reaction mixture was filtered through a fine porosity frit. The solvent was removed under reduced pressure, and the remaining pink solid was extracted in toluene and filtered again through a Celite containing pipet. The solution was concentrated, and bright pink crystals (139 mg, 82%) were obtained after cooling at −20 °C for 16 hours. ^{1}H NMR (C_6D_6, 600 MHz, 298K): 2.11 (s, 3H, CH_3), 3.08 (s, 30H, C_5**Me**$_5$), 6.61 (bs, 2H, *m*-(S)PhMe), 6.84-7.05 (m, 15H, P**Ph**$_3$), 7.98 (bs, 2H, *o*-(S)PhMe) ^{13}C NMR (C_6D_6, 150 MHz, 298K): 9.14 (s, (S)Ph**Me**), 22.1 (s, C_5**Me**$_5$), 125.7 (s, *p*-(S)PhMe), 128.5 (s, **C$_5$**Me_5), 129.7 (bs,(S)PhMe), 129.9 (s, (S)PhMe), 140.7 (bs, *ipso*-(S)PhMe), 150.9 (d, 2.8 Hz, *ipso*-PPh_3). Elemental analysis calculated for $C_{46}H_{52}CeO_2PS$: (840.07 g/mol): C, 65.77%; H 6.24%; S, 3.82%. Found: C, 65.38%; H, 6.08%; S, 3.67%.

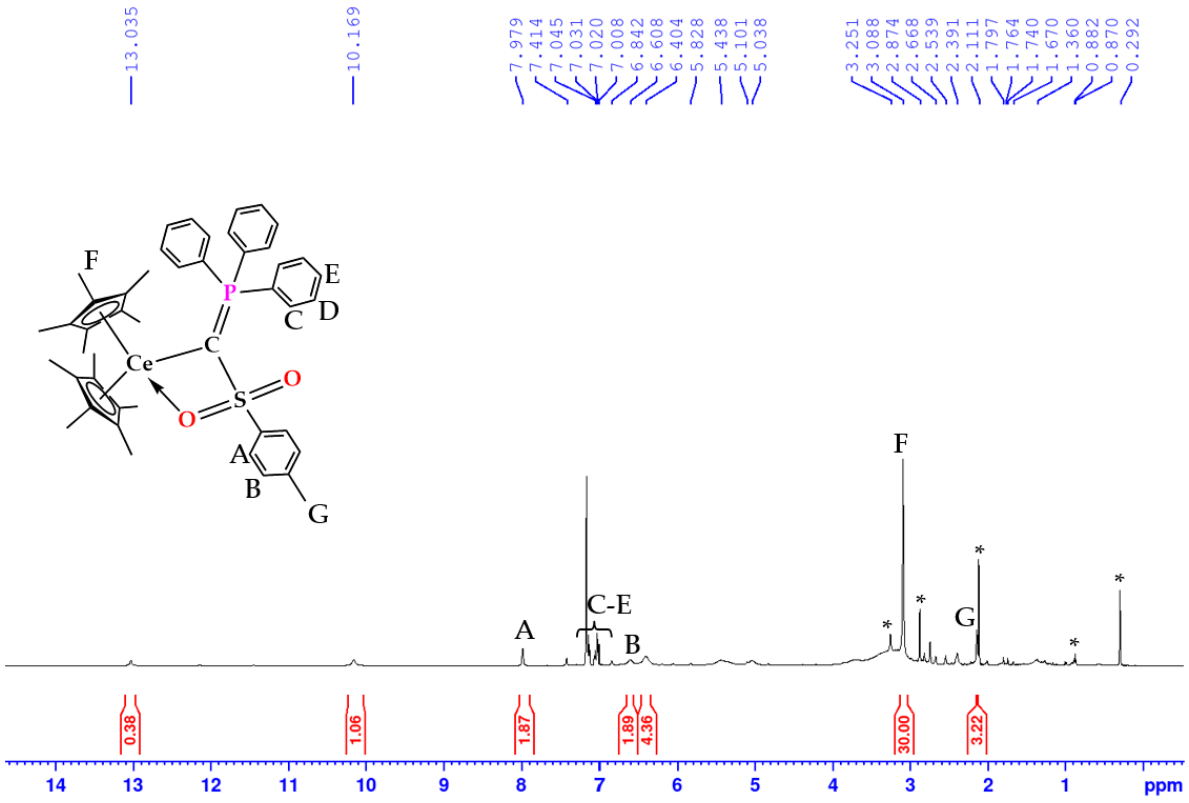

Figure S7: ^{1}H NMR (600 MHz, C_6D_6 298 K) of **2**. Solvent impurities are shown with (*).

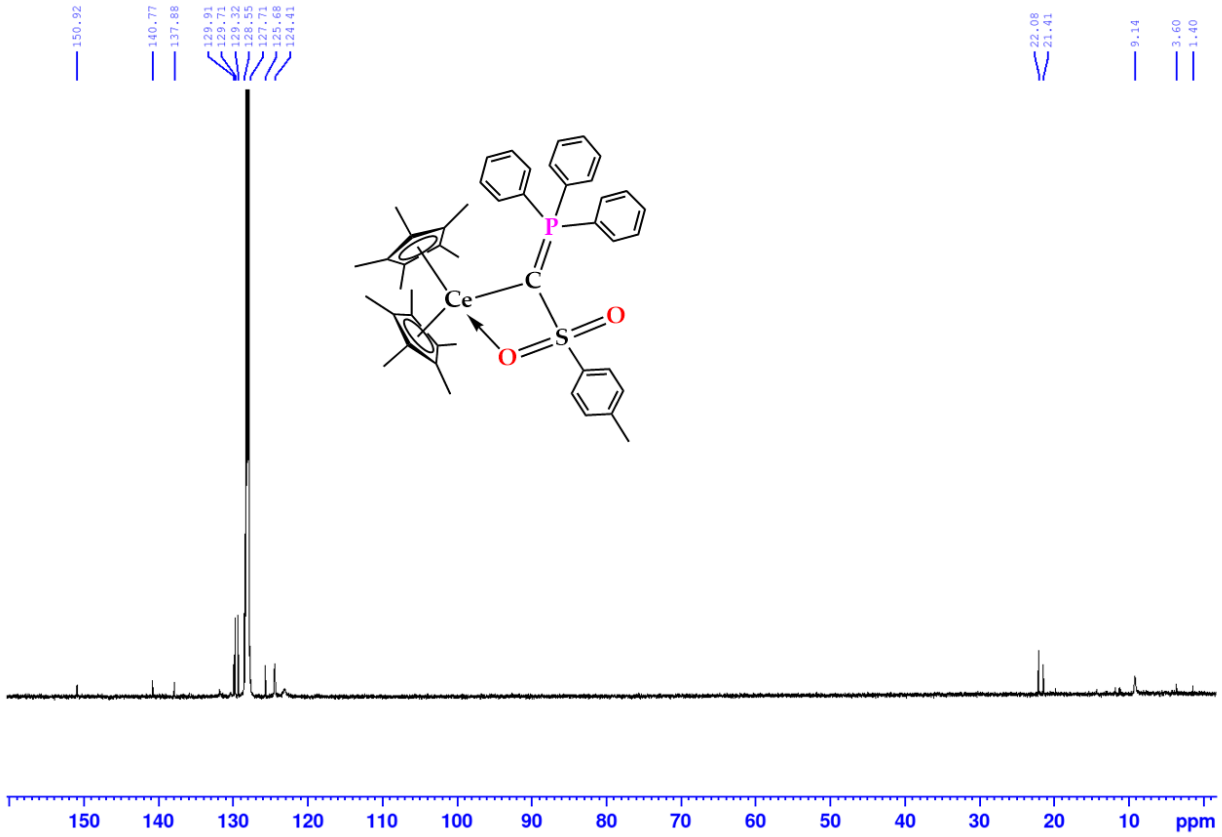

Figure S8: $^{13}C\{^{1}H\}$ NMR (120 MHz, C_6D_6 298 K) of **2**.

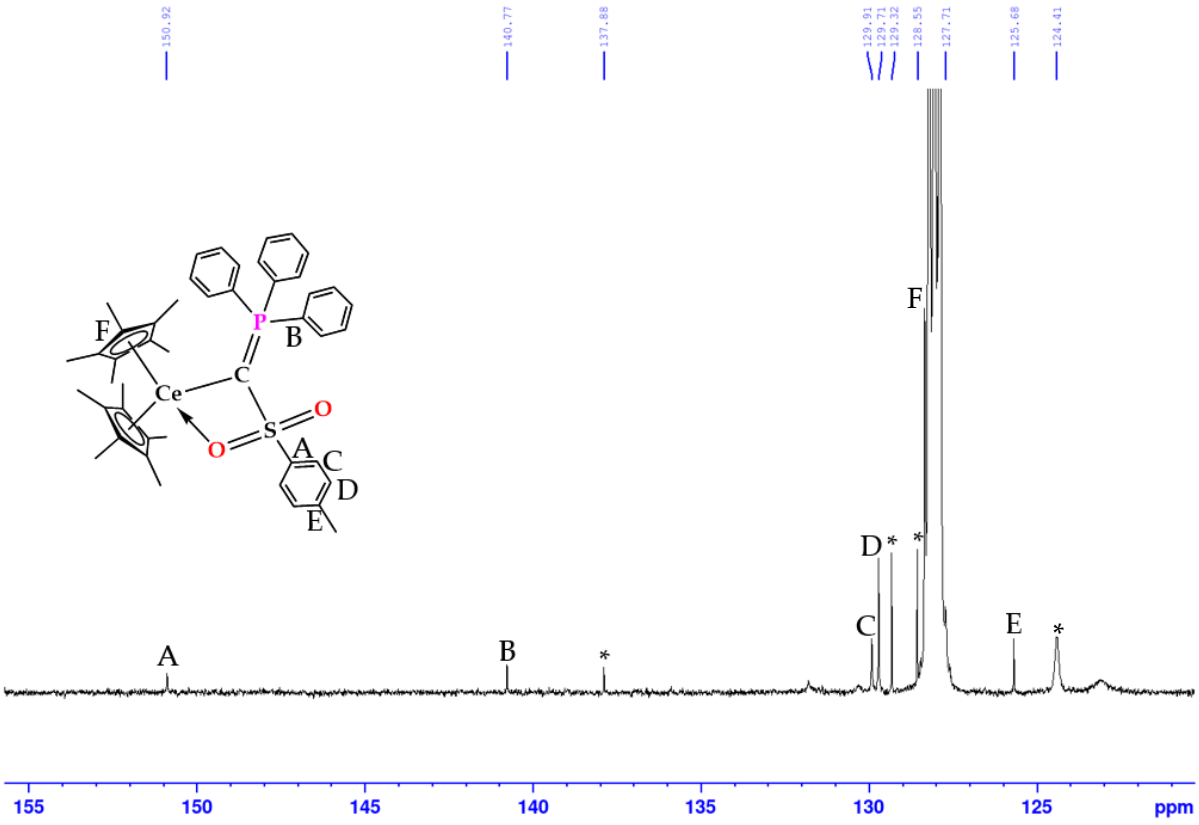

Figure S9: $^{13}C\{^{1}H\}$ NMR (120 MHz, C_6D_6, 298 K) of **2**, aryl region magnification, Ph_3P aryls are occluded by the solvent peak and toluene is present.

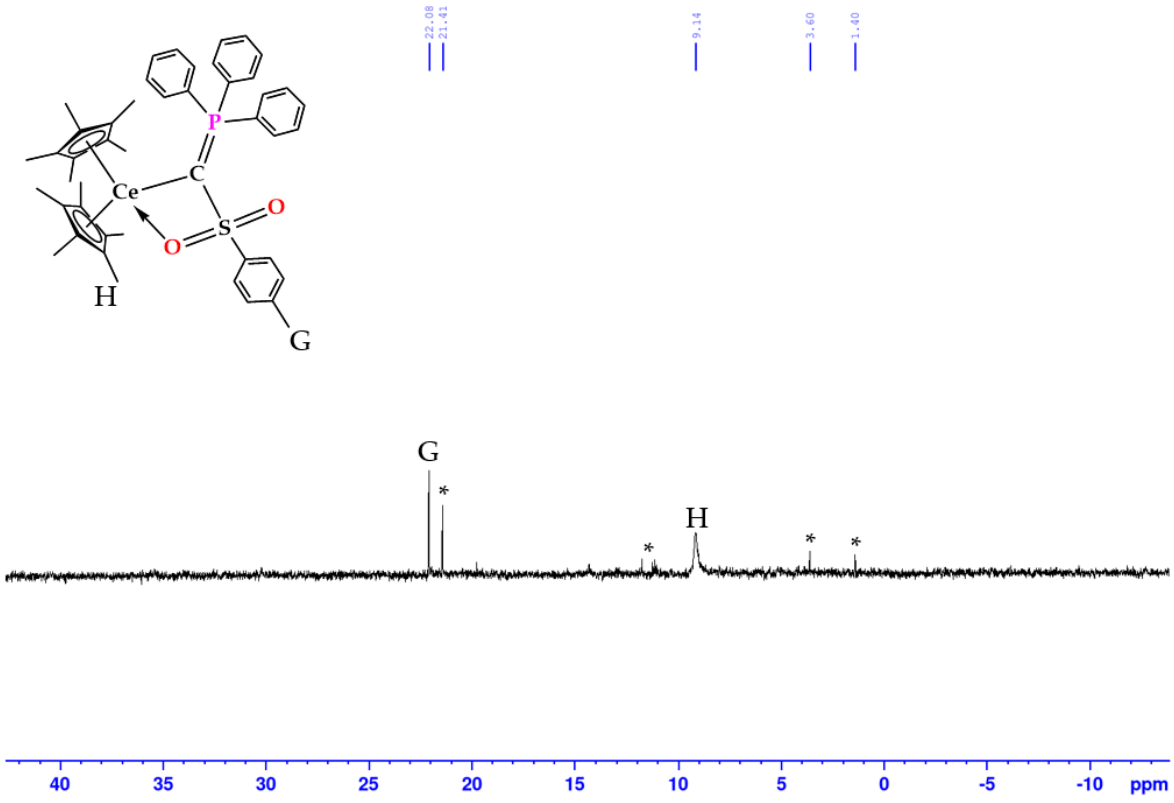

Figure S10: $^{13}C\{^{1}H\}$ NMR (120 MHz, C_6D_6 298 K) alkyl region magnification of **2**, impurities of toluene, *n*-pentane, and silicon grease are present.

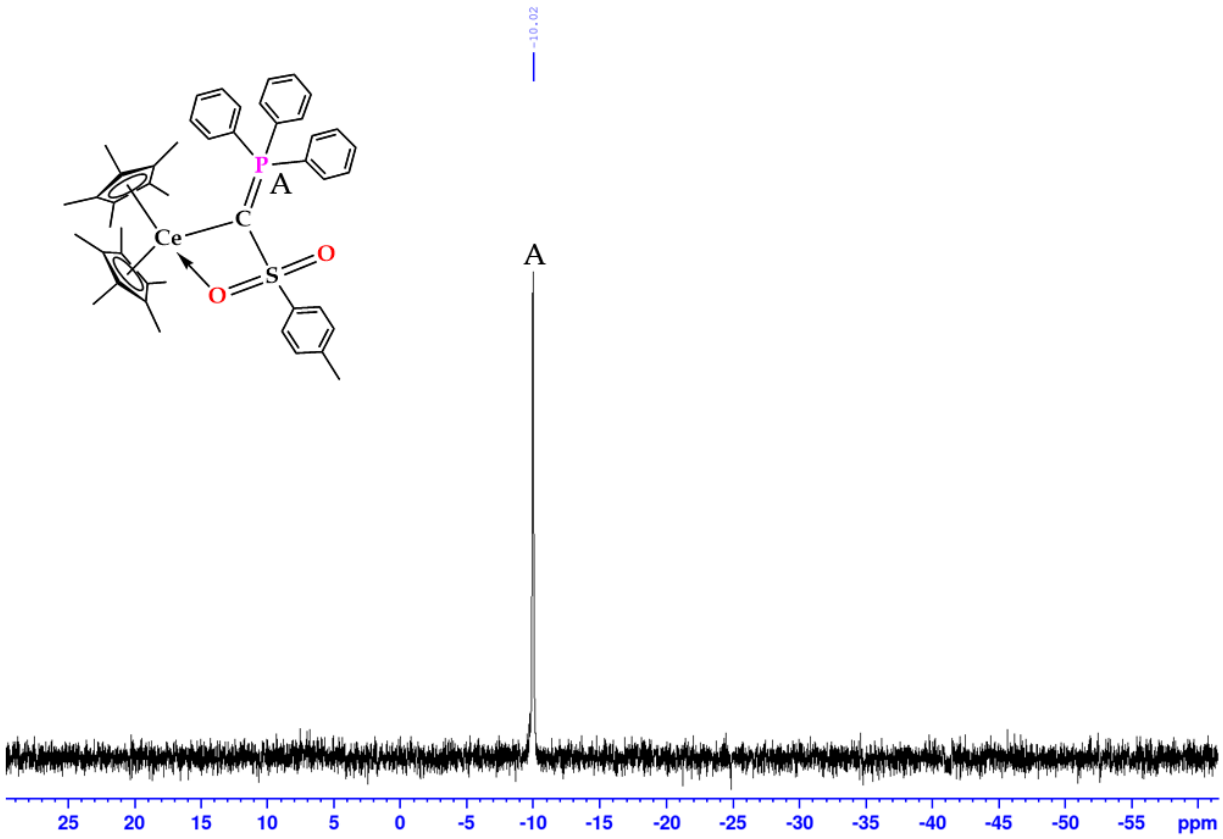

Figure S11: $^{31}P\{^{1}H\}$ NMR (150 MHz, C_6D_6 298 K) of **2**.

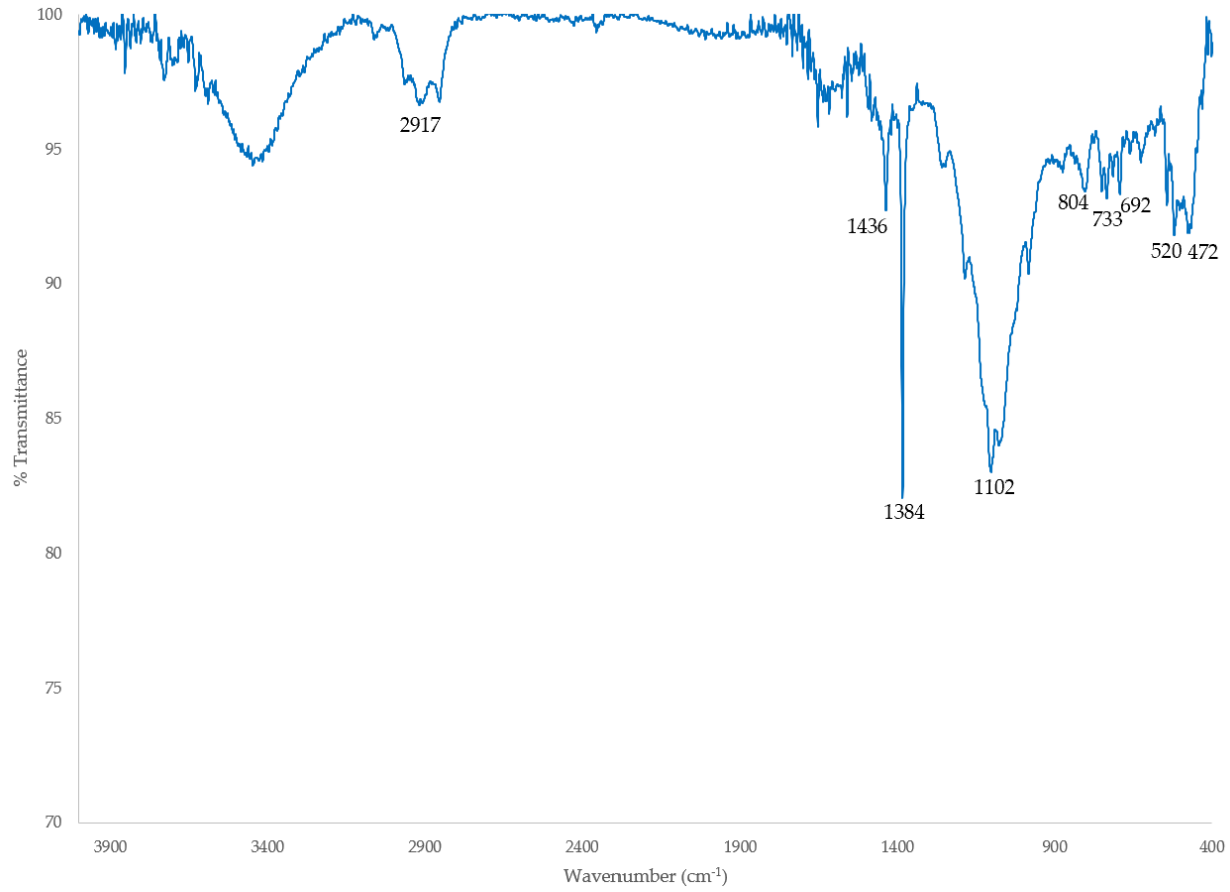

Figure S12: FT-IR vibrational spectrum of **2** obtained as a KBr pellet.

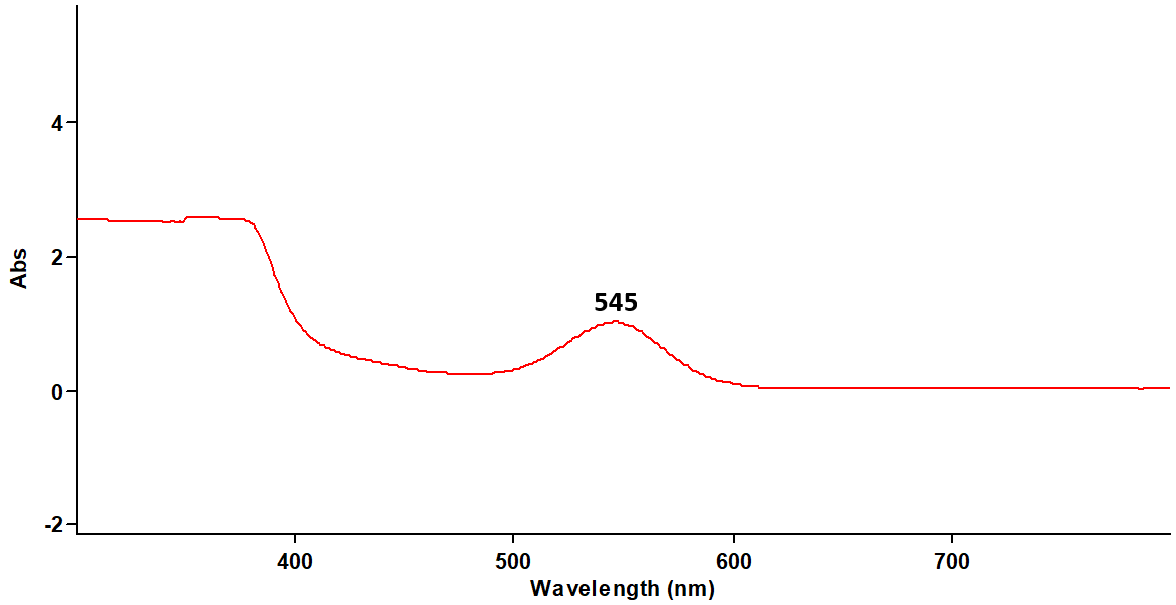

Figure S13: UV-vis spectrum of **2** (10 mM) in *n*-pentane with background subtraction.

Synthesis of [(C_5Me_5)$_2$Ce(κ^2-(C,S)-CCO{(S)PPh_2)}]$_2$, 3. [(C_5Me_5)$_2$Ce(κ^2-(C,S)-C(PPh_3){P(S)Ph_2}))], **1**, (120 mg, 0.133 mmol) was dissolved in tetrahydrofuran yielding a dark pink solution (20 mL) and added to a 100 mL Schlenk bomb flask. Following three freeze-pump-thaw cycles, an excess of CO was added (1 atm), resulting in the formation of a light-yellow solution. After 16 hours of stirring at room temperature, the solution was filtered through celite, and the volume was reduced in vacuo to ca. 5 mL and layered with n-pentane. Dark yellow crystals formed at the solvent layering interface after storage at -15 °C (62 mg, 70%). ^{1}H NMR (C_6D_6, 600 MHz, 298K): -1.60 (s, 2H, *p*-PPh_2), 3.98 (s, 30H, C_5**Me**$_5$), 5.12 (bs, 4H, *m*-PPh_2), 5.98 (bs, 2H, *o*-PPh_2) ^{13}C{^{1}H} NMR (C_6D_6, 150 MHz, 298K): 11.1 (s, C_5**Me**$_5$), 128.4 (s, **C**$_5$$Me_5$), 128.8 (d, 9 Hz, *ipso*-PPh_2), 129.4 (bs, PPh_3), 131.4 (d, C**C**O), 133.5 (m, PPh_2), 134.2 (d, 18 Hz, **C**CO) 138.2 (d, 10.8 Hz, *ipso*-PPh_2). %). ^{31}P{^{1}H} MR (C_6D_6, 150 MHz, 298K): -121.8 (s, **P**Ph_2). Elemental analysis calculated for $C_{35}H_{40}CeOPS$: (679.85 g/mol): C, 61.83%; H, 5.93%; S 4.72%. Found: C, 61.51%; H, 6.32%; S, 4.56%.

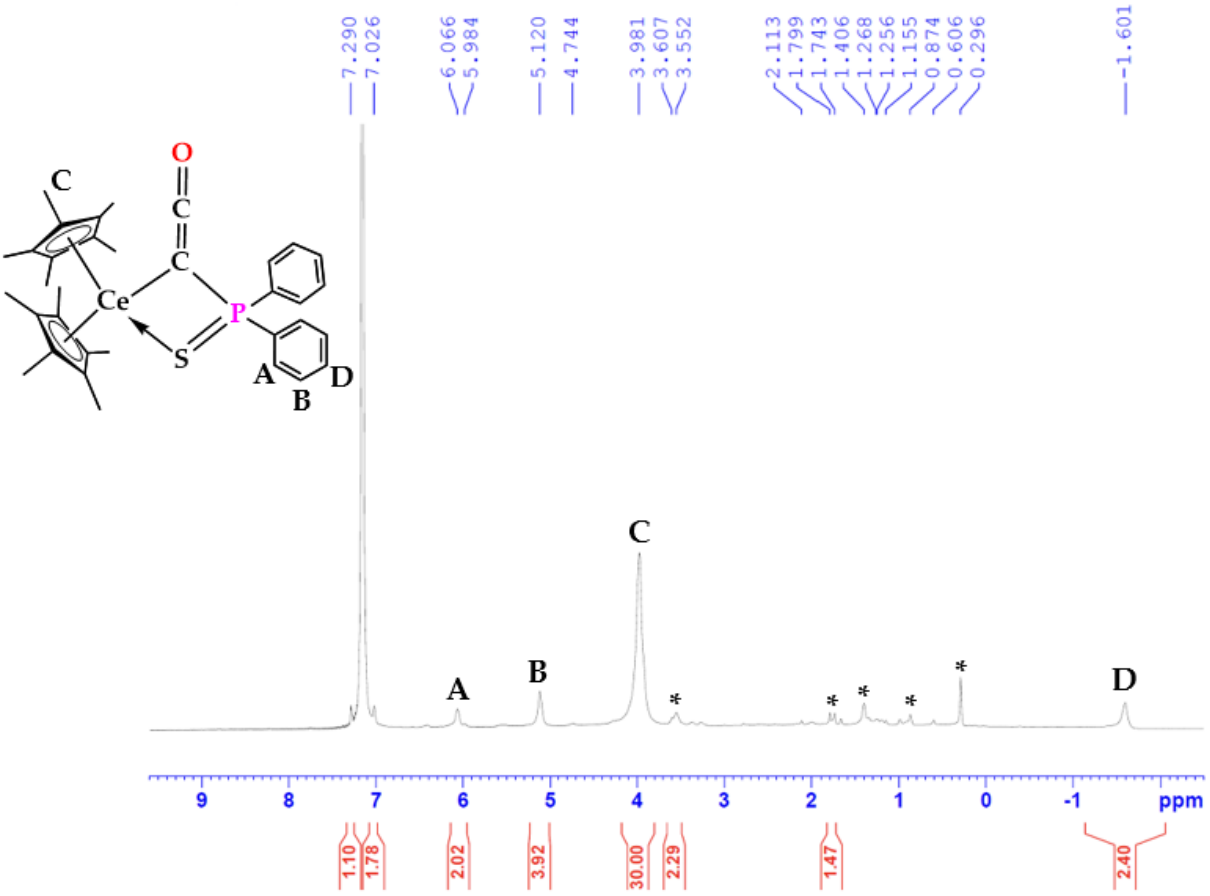

Figure S14: ^{1}H NMR (600 MHz, C_6D_6, 298 K) of **3** solvent impurities are present (toluene, *n*-pentane, silicon grease, THF).

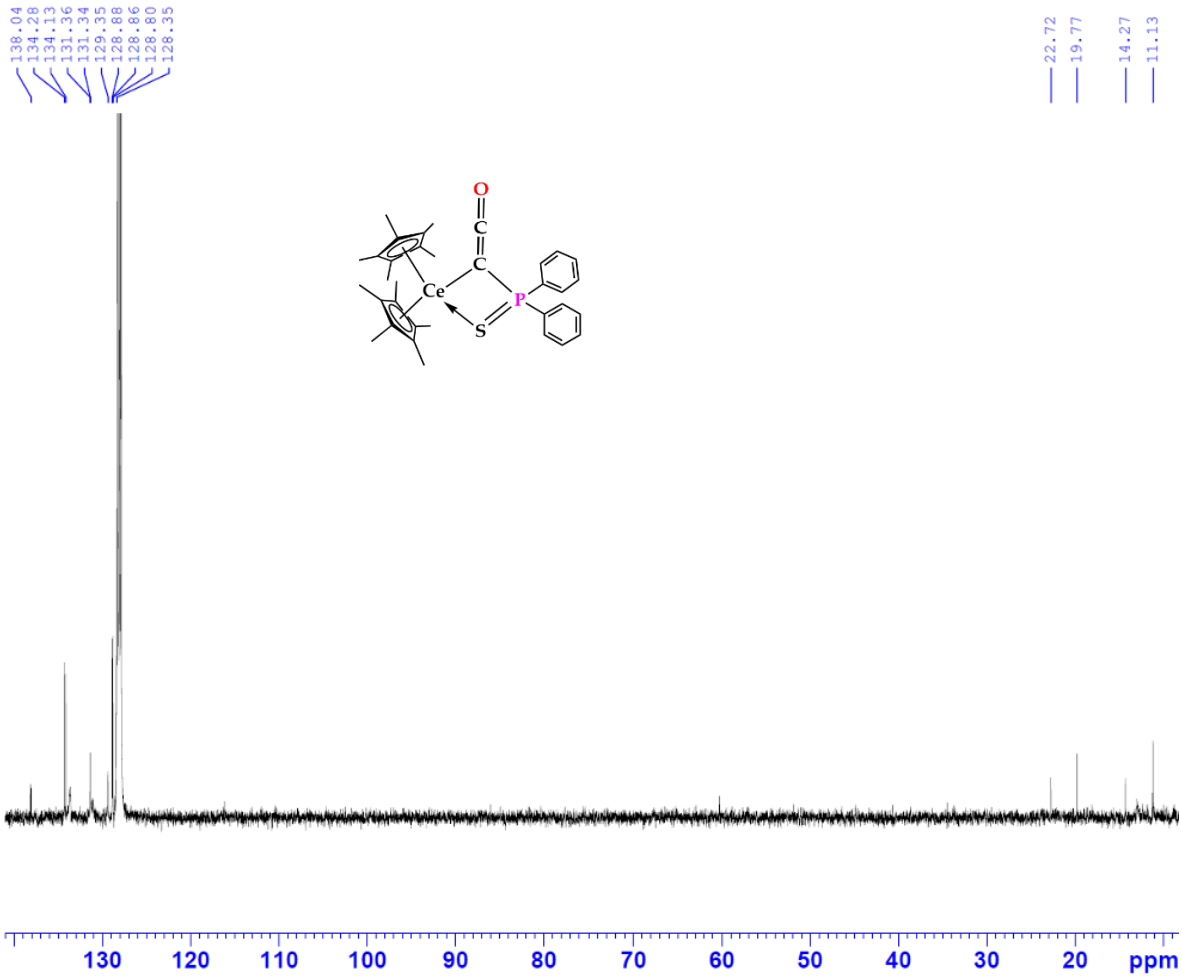

Figure S15*:* $^{13}C\{^{1}H\}$ NMR (120 MHz, C_6D_6 298 K) of **3**.

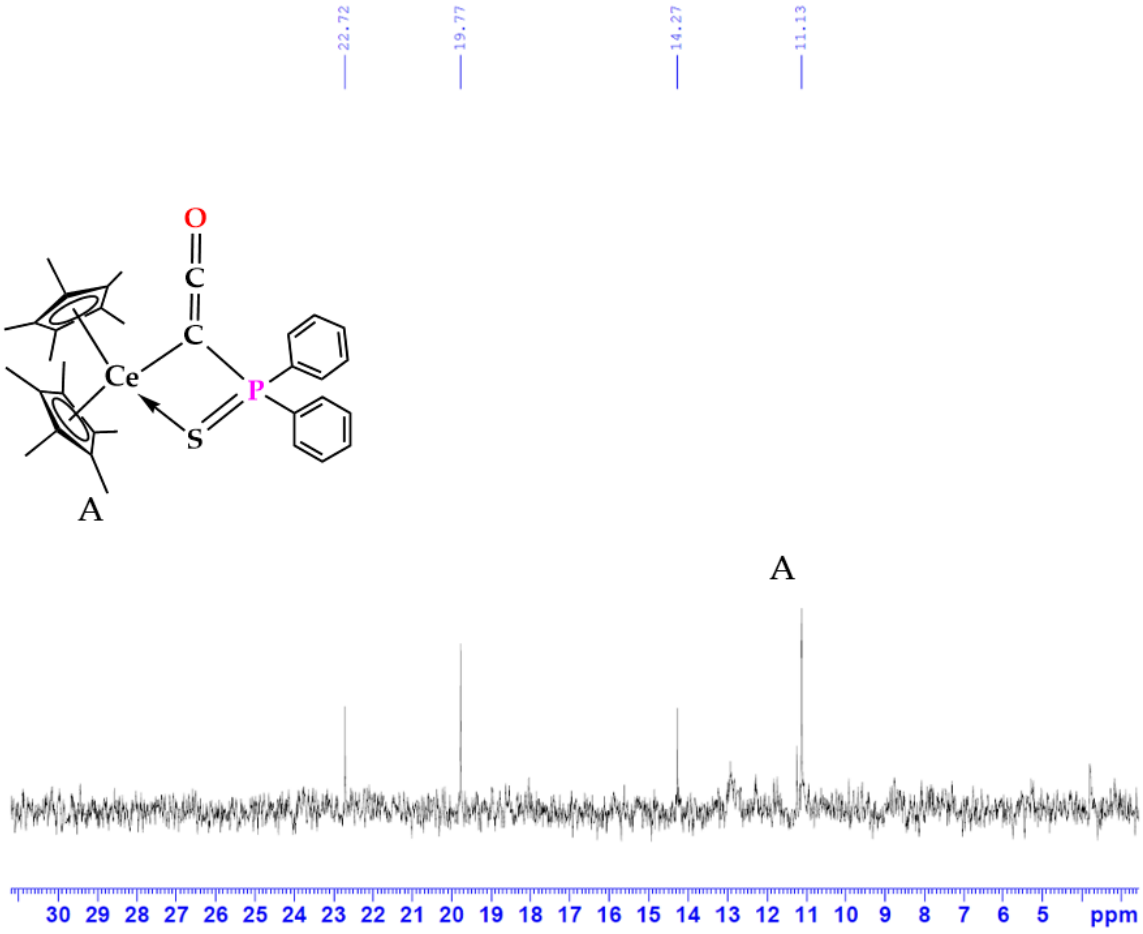

Figure S16*:* $^{13}C\{^{1}H\}$ NMR (120 MHz, C_6D_6 298 K) of **3**, alkyl region magnification, toluene and *n*-pentane are present as solvent impurities.

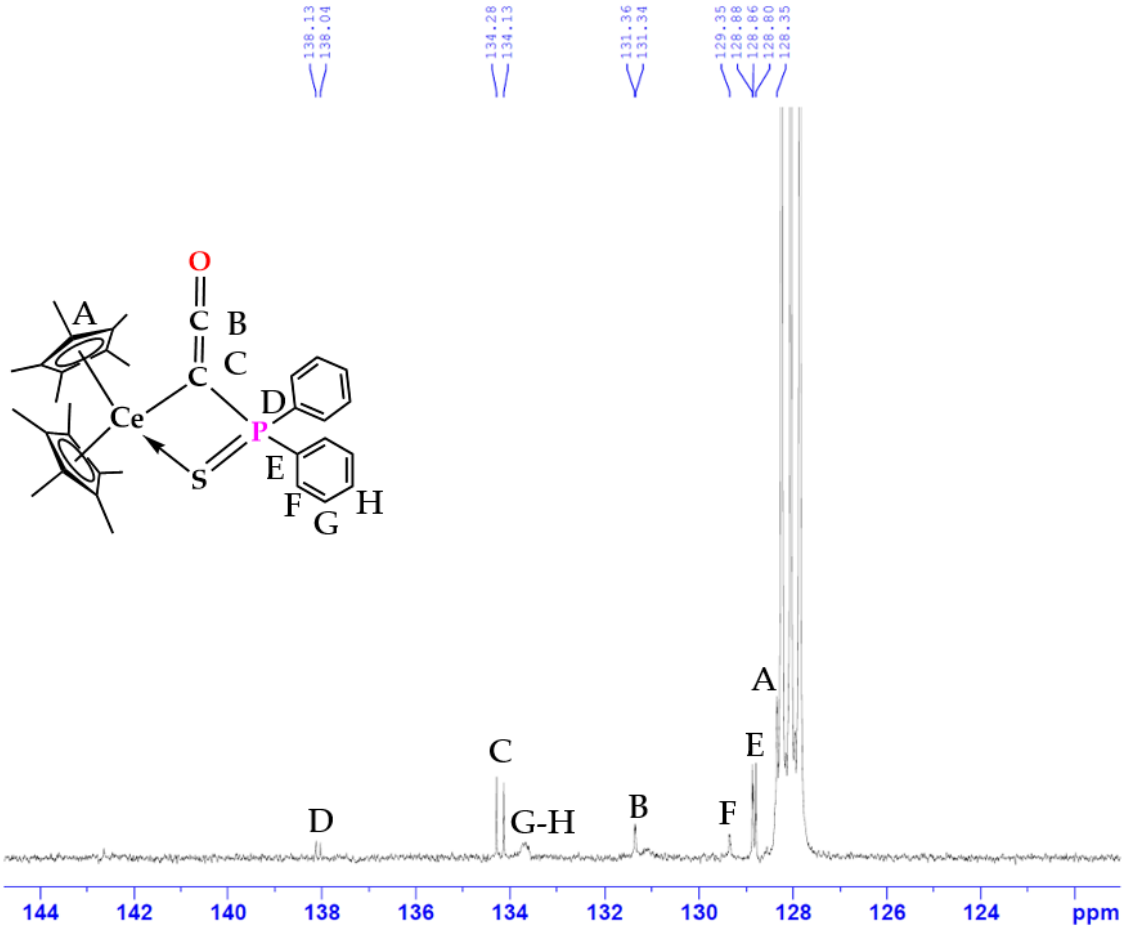

Figure S17*:* $^{13}C\{^{1}H\}$ NMR (120 MHz, C_6D_6 298 K) of **3**, aryl region magnification.

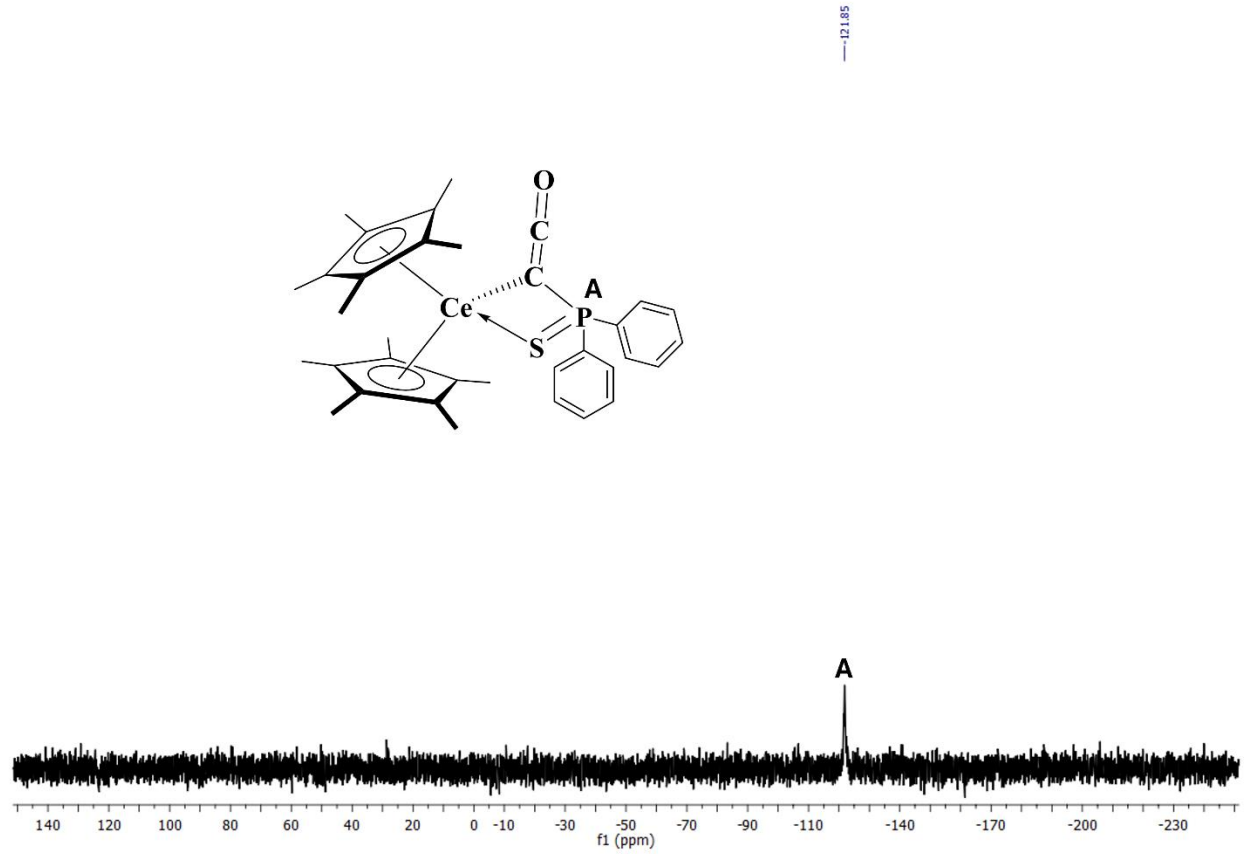

Figure S18: $^{31}P\{^{1}H\}$ NMR (150 MHz, C_6D_6 298 K) of **3**.

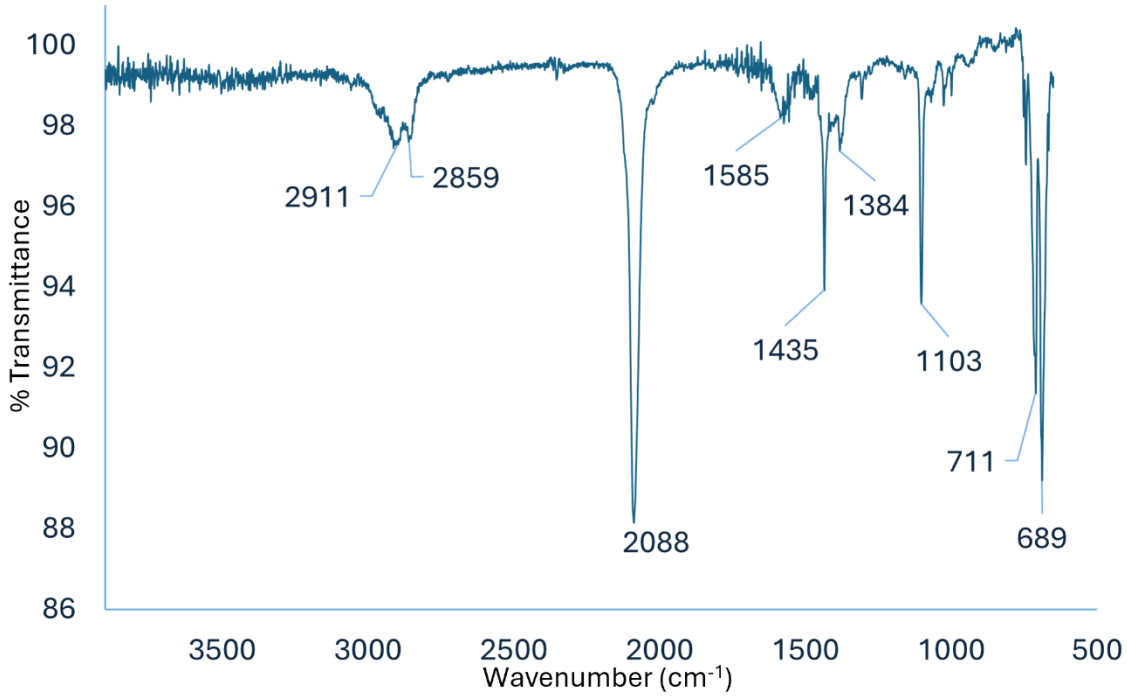

Figure S19: FT-IR vibrational spectrum of **3**, obtained using ATR.

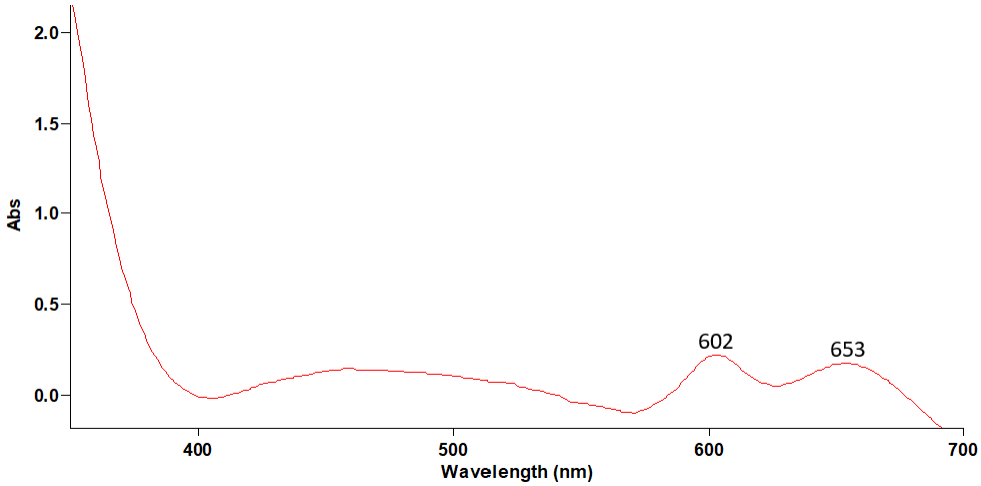

Figure S20: UV-vis spectrum of **3** (10 mM) in THF with background subtraction.

Synthesis of [$(C_5Me_5)_2Ce(SO_2PhMe)]_2$, 4. [$(C_5Me_5)_2Ce(\kappa^2$-(C,O)-C($PPh_3$){($SO_2PhMe$})], **2**, (100 mg, 0.119 mmol) was dissolved in toluene (10 mL) and added to a 100 mL Schlenk bomb flask. Following three freeze-pump-thaw cycles, an excess of CO was added (1 atm), resulting in the formation of a light-yellow solution. After stirring at room temperature for 16 h, the reaction mixture was filtered through a fine porosity frit. The solvent was removed under reduced pressure, and the remaining yellow solid was extracted in toluene and filtered again through a Celite containing pipet. The solution was concentrated, and light-yellow crystals (87.5 mg, 65%) were obtained after cooling at −20 °C for 16 hours. ^{1}H NMR (C_6D_6, 600 MHz, 298K): -1.60 (s, 2H, *p*-PPh_2), 3.35 (s, 30H, C_5**Me**$_5$). $^{31}P\{^1H\}$ NMR (C_6D_6, 150 MHz, 298K): 2.86 (s, Ph_3**P**CCO), 13.8 (s, SO_2CH**P**Ph_3). Elemental analysis calculated for $C_{54}H_{74}Ce_2O_4S_2$: (1131.53 g/mol): C, 57.32%; H 6.59% S 5.67%. Found: C, 57.38%; H, 6.55%; N 0.00%; S 5.25%.

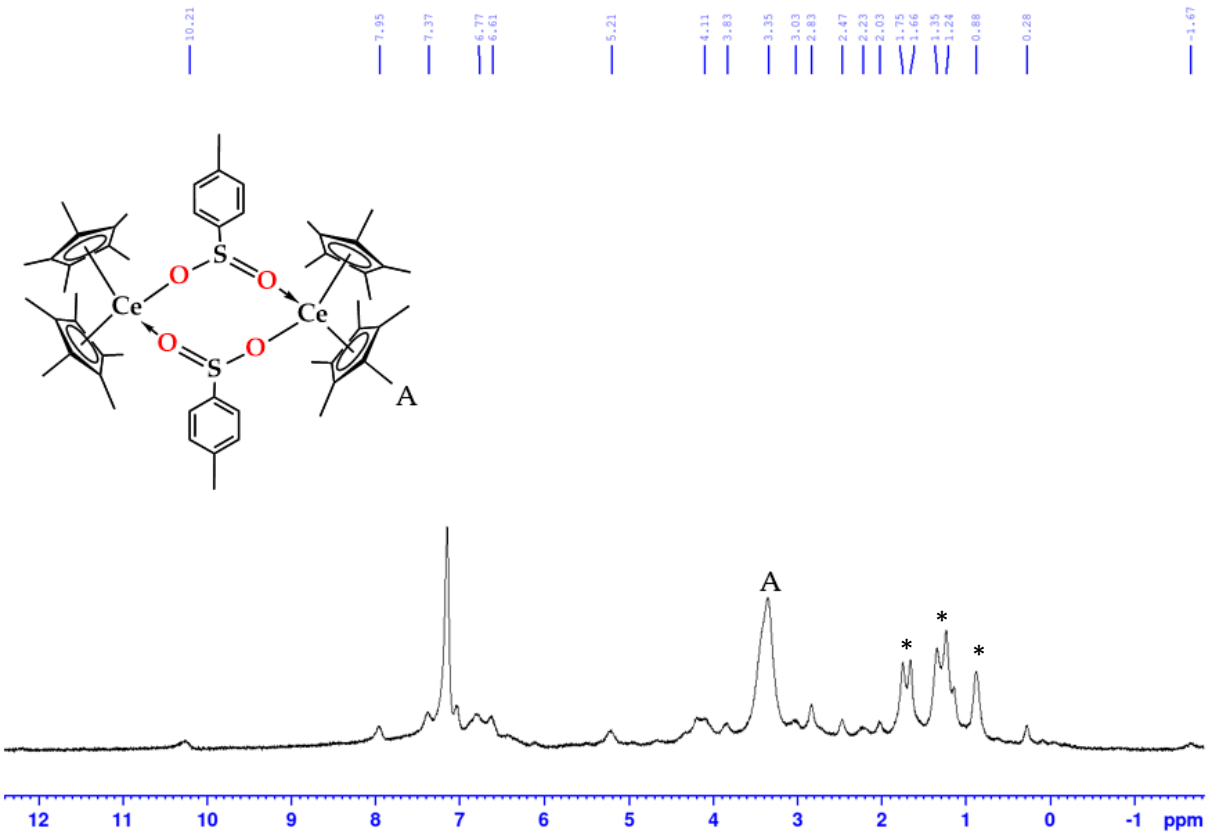

Figure S21: ^{1}H NMR (600 MHz, C_6D_6 298K) of **4**, silicon grease, *n*-pentane and THF are present as solvent impurities.

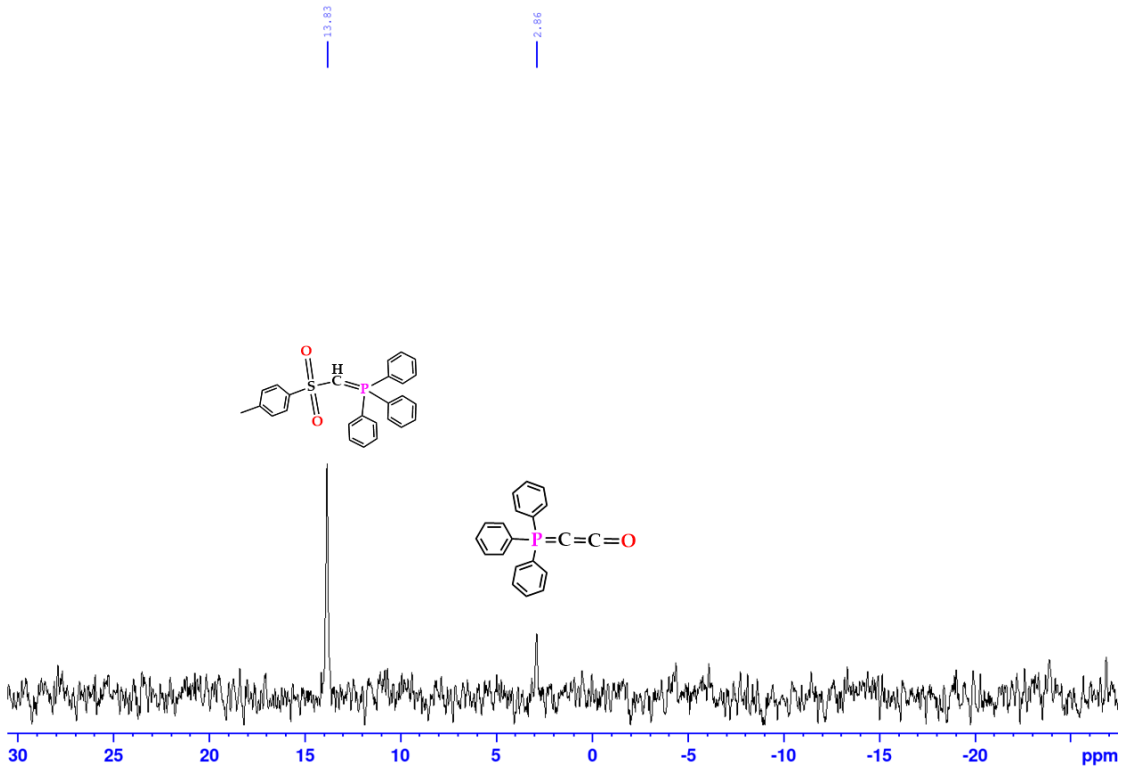

Figure S22: $^{31}P\{^{1}H\}$ NMR (150 MHz, C_6D_6 298 K) of the crude reaction to form **4**, protonated ylide carried through the synthesis is visible alongside Bestmann's ylide (2.86 ppm).

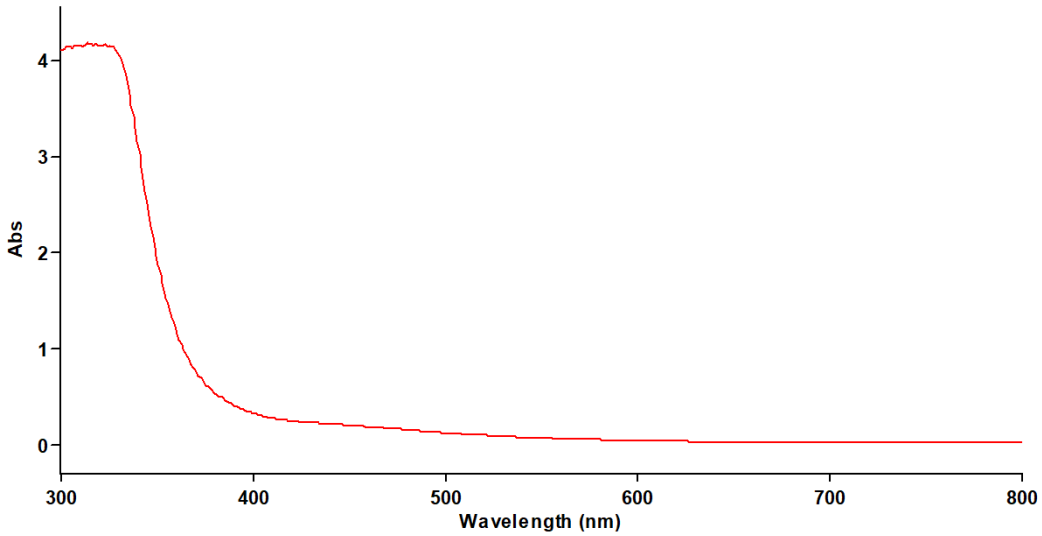

Figure S23: UV-vis spectrum of **4** (10 mM) in THF with background subtracted, the previously observed peak in the 500-600 range is conspicuously absent with loss of the yldiide ligand.

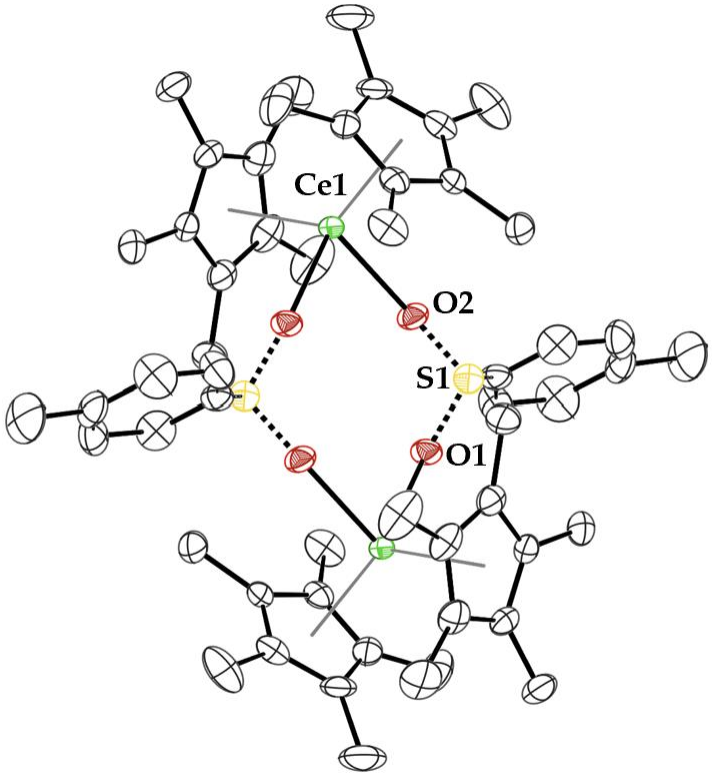

Figure S24. Molecular structure of **4** shown at the 50% probability level. The hydrogen atoms have been omitted for clarity.

Computational details.

All DFT calculations were carried out with the Gaussian 09 suite of programs.[5] Geometries were fully optimized in gas phase without symmetry constraints, employing the B3PW91 functional.[6,7] The nature of the extrema was verified by analytical frequency calculations. The calculation of electronic energies and enthalpies of the extrema of the potential energy surface (minima and transition states) were performed at the same level of theory as the geometry optimizations. IRC calculations were performed to confirm the connections of the optimized transition states. Cerium atoms were treated with a core effective core potential (46 MWB), associated with its adapted basis set.[8,9] For the other elements (S, H, O, P and C), Pople's double-ζ basis set 6-31G(d,p) was used.[10-12] The electronic charges (at the DFT level) were computed using the natural population analysis (NPA) technique.[13]

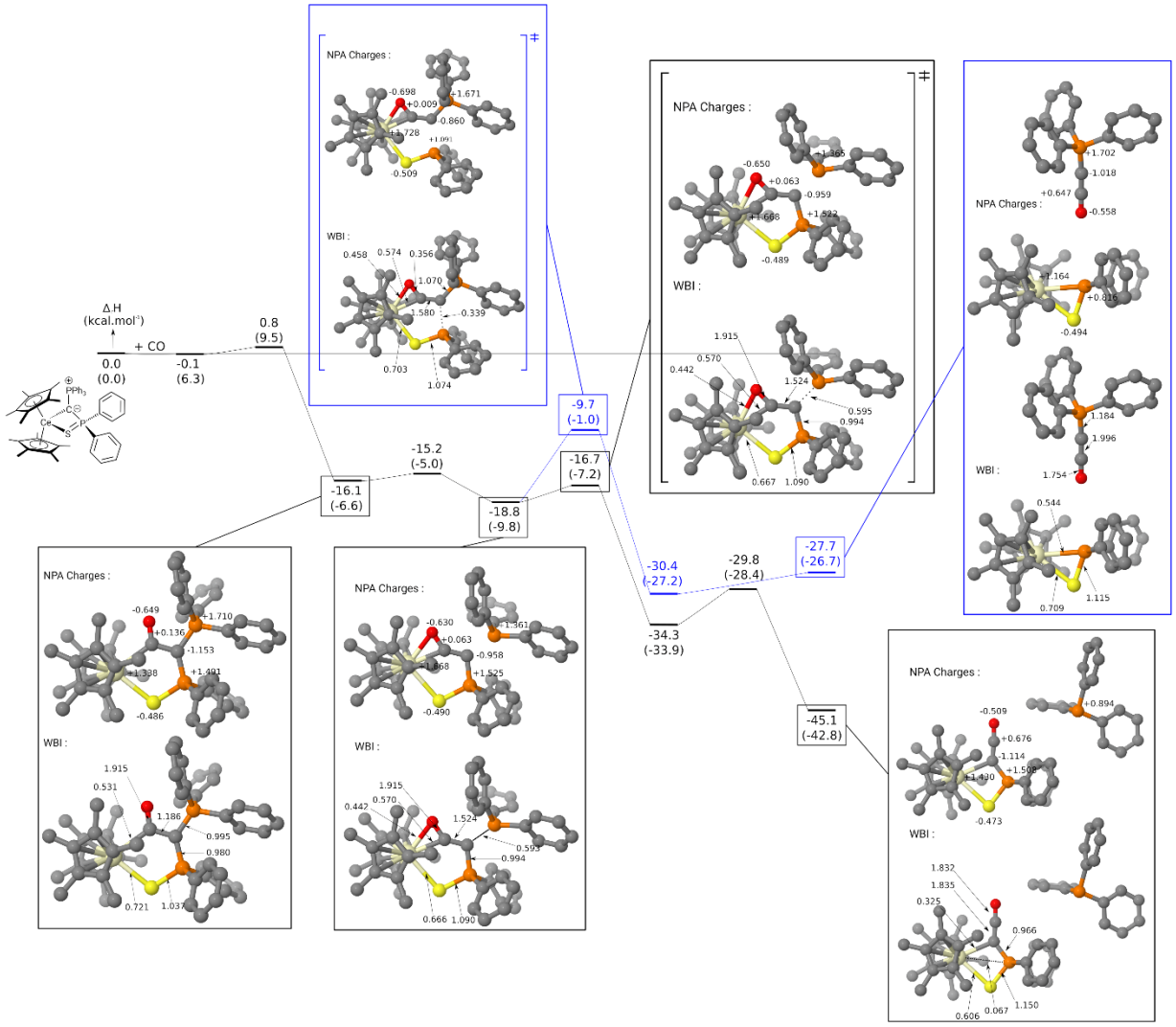

Figure S25. Reaction profile of **1** with CO showing the formation of the ketenyl complex, **3**.

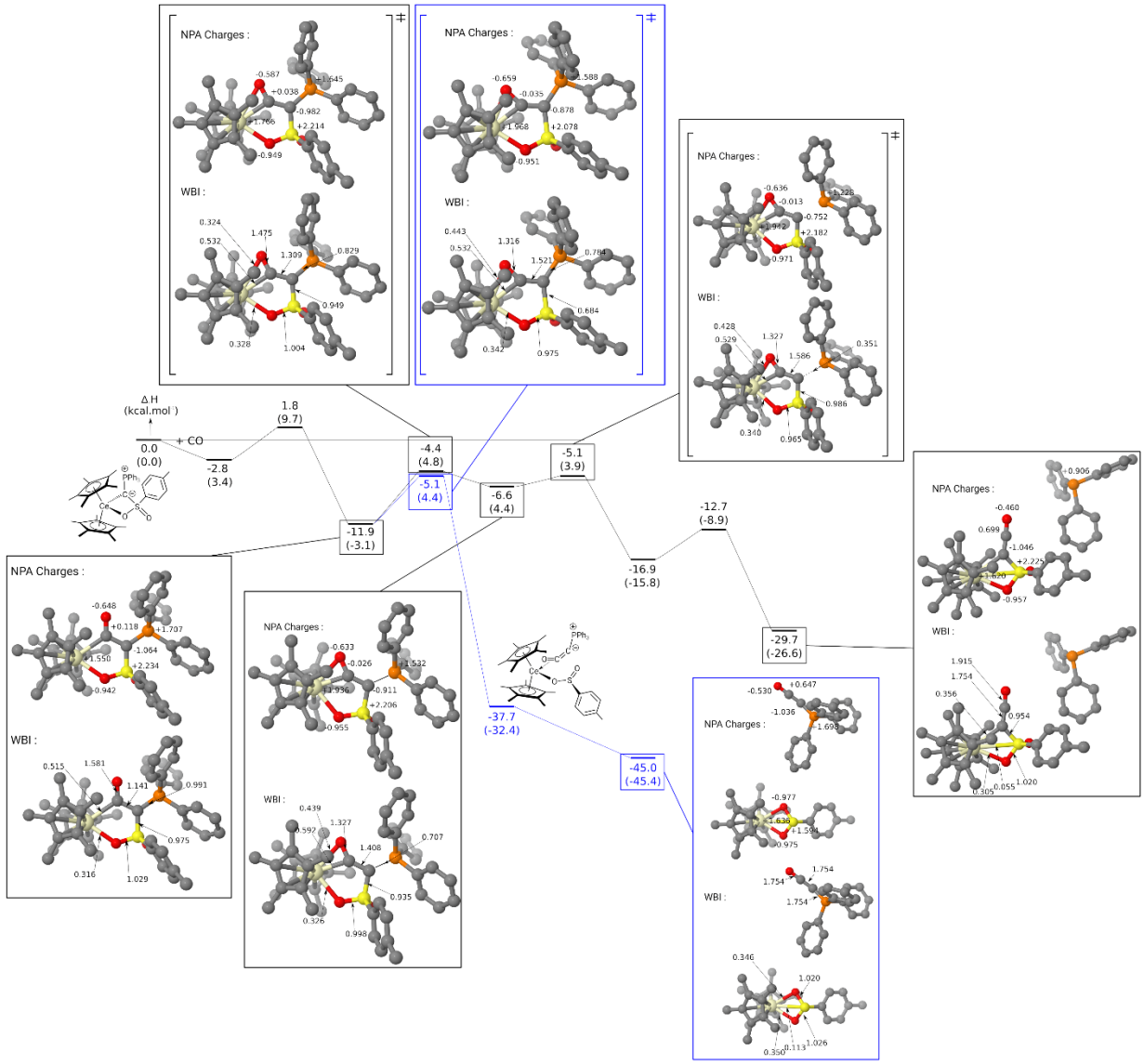

Figure S26. Reaction profile of **2** with CO showing the formation of the sulfonyl complex, **4**.

Crystal Structure Refinement. Single crystal X-ray diffraction data (SCXRD) were collected on a Bruker D8 Venture diffractometer equipped with a Photon II CMOS area detector using Mo-Kα radiation (λ = 0.71078 Å) from a microfocus source (Bruker AXS, Madison, WI, USA). Crystals were cooled to their collection temperatures under a stream of N_2 gas using a Cryostream 800 cryostat (Oxford Cryosystems, Oxford, UK). Hemispheres of unique data were collected using strategies of scans about the phi and omega axes. Data sets for **2** and **4** were integrated as two-component twins. Unit cell determination, data collection, data reduction, absorption correction and scaling, and space group determination were done using the Bruker Apex4 software suite.[14]

The crystal structures of **1·0.5C$_7$H$_8$** and **2** were solved by an iterative dual space approach as implemented in SHELXT.[15] The structures of **3, 4,** and **1·O(CH$_2$CH$_3$)$_2$** were solved by direct or Patterson methods as implemented in SHELXS.[16] Structures were refined by full-matrix least squares refinement against $|F^2|$ using SHELXL v.2018.[17] Full-occupancy non-hydrogen atoms were refined anisotropically. Disordered toluene molecules on centers of inversion were located from the difference map in both **1** and **2**. Hydrogen atoms were placed in calculated positions and constrained to ride on the carrier atoms; hydrogen atoms on methyl groups were also allowed to rotate about the H_3C-C bond axis. Olex2 was used as a graphical interface for model building.[18]

For **1·0.5C$_7$H$_8$** the best diffracting specimen that could be obtained was a fragment of a polycrystalline film which produced extraneous diffraction peaks that could not be indexed. Treating this crystal as a single domain produced a satisfactory refinement in which all full occupancy non-hydrogen atoms could be refined anisotropically without restraint. The final model contains large residual difference map peaks and high R_{int} and R_1 values which are due to contamination from the other crystal domains. The structure also has a large negative peak near the Ce atom; mononuclear organometallic structures commonly have packing faults which cause the heaviest atoms to behave as though they are positionally disordered which would account for this. These artifacts can potentially make elemental assignment ambiguous and introduce errors in bond distance, but the agreement with the other structurally characterized examples in this study indicates that the most important structural features are not affected by error. **1·0.5C$_7$H$_8$** contains a toluene molecule of crystallization disordered about a center of inversion

which was refined isotropically. The structure of **1** in **1·0.5C$_7$H$_8$** is almost identical to the more reliable refinement of **1·O(CH$_2$CH$_3$)$_2$**, which further verifies the atom assignments in **1·0.5C$_7$H$_8$**.

Table S1. Crystallographic parameters for complexes **1**-**4**.

	1·0.5(OEt$_2$)	**1·0.5C$_7$H$_8$**	**2·0.5C$_7$H$_8$**	**3**	**4**
CCDC number	2394687	2362374	2362375	2362376	2362377
Chemical formula	$C_{55}H_{55}P_2SCe$	$C_{54.50}H_{59}P_2SCe$	$C_{49.50}H_{56}O_2PSCe$	$C_{68}H_{80}O_2P_2S_2Ce_2$	$C_{54}H_{74}O_4S_2Ce_2$
Formula weight (g/mol))	976.19	948.13	886.09	1335.62	1131.49
Crystal habit/color	Triangular Prism/Red	Plate/Red	Fragment/Pink	Needle/Yellow	Plate/Yellow
Temperature (K)	173.0(1)	173.0(1)	173.0(1)	173.0(1)	173.0(1)
Space group	$P2_1/c$	P-1	P-1	P-1	$P2_1/c$
Crystal system	Monoclinic	Triclinic	Triclinic	Triclinic	Monoclinic
Volume (Å^3)	4838.7(2)	2330.8(4)	2116.68(14)	1544.49(13)	2592.9(2)
a (Å)	18.6645(5)	11.1322(12)	10.2451(4)	12.0893(6)	10.4042(5)
b (Å)	13.3611(4)	12.2852(13)	12.2641(5)	12.1740(6)	10.5714(5)
c (Å)	19.5603(6)	18.985(2)	18.6768(7)	12.3858(6)	23.8222(11)
α (deg)	90	94.316(4)	98.6100(10)	115.1891(16)	90
β (deg)	97.268(1)	103.713(4)	92.8490(10)	99.9137(17)	98.2743(16)
γ (deg)	90	110.258(4)	113.2370(10)	101.7517(17)	90
Z	4	2	2	1	2
Calculated density (g/cm^3)	1.340	1.351	1.390	1.436	1.449
Absorption coefficient (mm^{-1})	1.088	1.125	1.201	1.617	1.856
Final *R* indices [$I > 2\sigma(I)$]	$R_1 = 0.0339$ $wR^2 = 0.0617$	$R_1 = 0.1159$ $wR^2 = 0.2560$	$R_1 = 0.0373$ $wR^2 = 0.0603$	$R_1 = 0.0611$ $wR^2 = 0.1210$	$R_1 = 0.0356$ $wR^2 = 0.0743$

References

1. Evans, W. J.; Olofson, J. M.; Zhang, H.; Atwood, J. L.. *Organometallics,* **1988**, *7* (3), 629–633.
2. Schlosser, M.; Hartmann, J., *Angew. Chem. Int. Ed.,* **1973**, *12* (6), 508–509.
3. Jörges, M.; Krischer, F.; Gessner, V. H., *Science* **2022**, *378* (6626), 1331–1336.
4. Scherpf, T.; Wirth, R.; Molitor, S.; Feichtner, K.-S.; Gessner, V. H., *Angew. Chem. Int. Ed.* **2015**, *54* (29), 8542–8546.
5. Gaussian 09. Revision D.01. M. J. Frisch. G. W. Trucks. H. B. Schlegel. G. E. Scuseria. M. A. Robb. J. R. Cheeseman. G. Scalmani. V. Barone. B. Mennucci. G. A. Petersson. H. Nakatsuji. M. Caricato. X. Li. H. P. Hratchian. A. F. Izmaylov. J. Bloino. G. Zheng. J. L. Sonnenberg. M.Hada. M. Ehara. K. Toyota. R. Fukuda. J. Hasegawa. M. Ishida. T. Nakajima. Y. Honda. O.Kitao. H. Nakai. T. Vreven. J. A. Montgomery. Jr.. J. E. Peralta. F. Ogliaro. M. Bearpark. J. J.Heyd. E. Brothers. K. N. Kudin. V. N. Staroverov. R. Kobayashi. J. Normand. K. Raghavachari. A. Rendell. J. C. Burant. S. S. Iyengar. J. Tomasi. M. Cossi. N. Rega. J. M. Millam. M. Klene. J. E. Knox. J. B. Cross. V. Bakken. C. Adamo. J. Jaramillo. R. Gomperts. R. E. Stratmann. O. Yazyev. A. J. Austin. R. Cammi. C. Pomelli. J. W. Ochterski. R. L. Martin. K. Morokuma. V. G. Zakrzewski. G. A. Voth. P. Salvador. J. J. Dannenberg. S. Dapprich. A. D. Daniels. Ö. Farkas. J. B. Foresman. J. V. Ortiz. J. Cioslowski. and D. J. Fox. Gaussian. Inc.. Wallingford CT. **2009**.
6. J. P. Perdew, J. A. Chevary, S. H. Vosko, K. A. Jackson, M. R. Pederson, D. J. Singh and C. Fiolhais, *Phys. Rev. B*, **1992**, 46, 6671-6687.
7. A. D. Becke, *J. Chem. Phys.*, **1993**, 98, 5648-5652.
8. M. Dolg, H. Stoll, H. Preuss, *J. Chem. Phys.* 1989, **90**, 1730 - 1734
9. X. Cao, M. Dolg, *J. Mol. Struct.* **2002**, ***581*,** 139 - 147
10. P. C. Hariharan and J. A. Pople, *Theor Chim Acta*, **1973**, 28, 213-222.
11. R. Ditchfield, W. J. Hehre and J. A. Pople, J. Chem. Phys., **1971**, 54, 724-728.
12. W. J. Hehre, R. Ditchfield and J. A. Pople, J. Chem. Phys., **1972**, 56, 2257-2261.
13. A. E. Reed, L. A. Curtiss and F. Weinhold, Chem. Rev., **1988**, 88, 899-926.
14. Apex4, AXScale, and SAINT, version 2022.1, Bruker AXS, Inc., Madison, WI, **2022**.
15. Sheldrick, G. M. *SHELXT* – Integrated space-group and crystal-structure determination. *Acta Cryst. Sect. A: Found. Adv.* **2015**, *71*, 3-8.
16. Sheldrick, G. M. SHELXS, v.2013-1, 2013.
17. Sheldrick, G. M. *SHELXT* – Integrated space-group and crystal-structure determination. *Acta Cryst. Sect. A: Found. Adv.* **2015**, *71*, 3-8.
18. Dolomanov, O.V.; Bourhis, L.J.; Gildea, R.J.; Howard, J.A.K.; Puschmann, H. *OLEX2:* A complete structure solution, refinement, and analysis program. *J. Appl. Cryst.* **2009**, *42*, 339-341.